Digital Object Identifier (DOI): 10.1109/TPEL.2017.2694455

IEEE Transaction on Power Electronics (Volume: 33, Issue: 3, March 2018)

Power routing for cascaded H-Bridge converters

Youngjong Ko
Markus Andresen
Giampaolo Buticchi
Marco Liserre

Suggested Citation

Y. Ko, M. Andresen, G. Buticchi and M. Liserre, "Thermally Compensated Discontinuous Modulation Strategy for Cascaded H-Bridge Converters," in *IEEE Transactions on Power Electronics*, vol. 33, no. 3, pp. 2704-2713, March 2018.

Thermally Compensated Discontinuous Modulation Strategy for Cascaded H-Bridge Converters

Youngjong Ko, *Student Member, IEEE*, Markus Andresen, *Student Member, IEEE*, Giampaolo Buticchi, *Senior Member, IEEE*, and Marco Liserre, *Fellow, IEEE*

***Abstract*—A widely adopted multilevel converter topology is the cascaded H-bridge (CHB), as it can provide voltage and power scalability. However, since the CHB converter can be composed by cells with different remaining lifetime, it could be useful to delay a fault of higher aged cells in order to prolong the entire converter's lifetime. In this paper, a thermally compensated discontinuous pulse width modulation (DPWM) strategy is proposed in order to reduce the thermal stress for power semiconductors in power modules of higher aged cells. Considering the thermal cycles as the most influencing cause of wear out of power modules, the proposed method compensates the thermal cycles under a varying power profile by manipulating the clamping angle of the DPWM. Moreover, the proposed method obtains a comparable total harmonic distortion performance to the phase-shifted carrier modulation.**

***Index Terms*—Active thermal control, cascaded H-bridge (CHB), discontinuous pulse width modulation (DPWM), multilevel converter, reliability.**

I. Introduction

MULTILEVEL converters have been widely adopted as an alternative to the two-level configuration in many high-voltage and high-power applications [1]–[3], because of their attractive features, such as reduced dv/dt, lower electromagnetic interference noise, smaller filter size and lower total harmonic distortion (THD) [4], [5]. Among the various multilevel topologies, the cascaded H-bridge (CHB) converter is commonly used in MV drives [6]–[8]. The higher number of components poses, however, more reliability problems than the nonmodular solution. This is an important issue in the power converter design in order to ensure uninterrupted operation. Although a modular structure can be made fault tolerant, this requires additional cells in the converter, addressing only the effect of a fault but not the root cause of the failure.

Manuscript received December 9, 2016; revised February 22, 2017; accepted April 9, 2017. Date of publication April 14, 2017; date of current version December 1, 2017. This work was supported in part by the European Union/Interreg V-A - Germany-Denmark, under PE: Region Project, and in part by the European Research Council under the European Union's Seventh Framework Programme (FP/2007-2013)/ERC Grant Agreement [616344] – HEART. This paper was presented in part at the *IEEE Applied Power Electronics Conference and Exposition*, Tampa, FL, USA, March 26–30, 2017. Recommended for publication by Associate Editor K. Ngo. *(Corresponding author: Youngjong Ko.)*

The authors are with the Chair of Power Electronics, Christian-Albrechts University of Kiel, Kiel 24143, Germany (e-mail: yoko@tf.uni-kiel.de; ma@tf.uni-kiel.de; gibu@tf.uni-kiel.de; ml@tf.uni-kiel.de).

Color versions of one or more of the figures in this paper are available online at http://ieeexplore.ieee.org.

Digital Object Identifier 10.1109/TPEL.2017.2694455

The reliability of a system needs to be analyzed based on the Physics-of-Failure (PoF) approach and power modules have been found to be one of the most frequent failure causes in power converters [9]. Several works based on the PoF approach have proved that the major failure mechanisms of power semiconductors in power modules are closely related to the thermal stress [10]–[12]. More precisely, the thermal cycling caused by power variations in a mission profile leads to accumulated fatigue, causing major failures such as the bond wire liftoff. Therefore, the reduction of thermal cycling can extend the lifetime of the converter [13].

In order to reduce the thermal cycling without over design or additional hardware, it is of interest to use active thermal control [14] for the improvement of the reliability. In [15]–[17], the switching frequency control method was presented, which manipulates the switching frequency depending on a power variation in order to reduce the thermal cycling. However, the adaptation of the switching frequency method usually causes a variation of the output current spectrum and a reduction of the switching frequency implies an increased THD, which is not acceptable in grid-connected applications. In order to comply with the regulations, this may require an over-designed filter. The power routing method in the modular converters was presented to redistribute the thermal stress among the cells depending on the expected remaining lifetime [18], [19]. The thermal cycling of a cell with lower expected lifetime can be reduced at the expense of increased stress for the other cells, which might not always be accepted. Finally, several papers claimed that the discontinuous modulation can improve the reliability by the reducing the switching losses [20], [21]. However, the THD of the current increases, which implies a requirement for a bigger output filter to satisfy the standards in grid-connected systems.

In this paper, the strategy based on discontinuous pulse width modulation (DPWM) is proposed, which performs the thermal cycling compensation with a good THD performance. In Section II, the features of the conventional carrier based modulation methods are reviewed before the motivation and the principle of the proposed method are described. Then, the loss distribution is demonstrated with the active clamping angle method. In Section III, the potential of the proposed method is discussed in terms of the number of cells and the modulation index and the THD performance is as well identified. The effect of the proposed method on the lifetime is simulated in Section IV. Before concluding this paper in Section VI, the proposed

method is implemented in the demonstrator and verified in terms of the thermal cycling compensation in Section V.

II. Thermally Compensated Discontinuous Modulation Strategy

A. Motivation and Principle

The conventional modulation schemes are reviewed before introducing the thermally compensated modulation. The conventional carrier-based modulation methods for CHB can be categorized in continuous or discontinuous modulation. More precisely, in accordance with the configuration of triangular carriers, the continuous modulation is divided into phase-shifted pulse width modulation (PS-PWM) and the level-shifted PWM (LS-PWM). The PS-PWM is realized with six triangular carriers, which have the same frequency and amplitude, but with a 60° phase displacement between adjacent carriers. The most attractive advantage of the PS-PWM is the six times higher equivalent switching frequency, which reduces the THD or the required filter size. However, more power losses are generated in the switching devices in comparison with the LS-PWM. By means of the LS-PWM, the losses can be significantly reduced with the reduced average switching frequency. However, since the losses are unevenly generated among cells, the switching pattern needs to be rotated [4].

The DPWM is generally utilized to reduce the switching losses by clamping the output voltage at either the positive or negative dc-link voltage. The losses can be significantly reduced in comparison with the PS-PWM because the power semiconductors are not switched during the clamping region. However, the THD of the current is increased due to the clamping behavior, requiring a bigger output filter or a higher switching frequency in comparison with the two continuous modulations introduced before [22], [23].

In the modular converter, each cell could have a different consumed lifetime, which may be caused by uneven stress during operation or by the failure of a cell and the consequent replacement [18]. To cope with the different lifetime of the cells, the proposal is a modulation strategy, which aims at delaying the failure of the most aged cells to extend the lifetime of the entire converter.

The proposed method has two kinds of modulation signals, as shown in Fig. 1, considering the single phase structure. The first modulation signal $v_{\text{ref},ns}$ shown in Fig. 1(a) has the clamping region, which is produced by the sum of the fundamental reference voltage $v_{\text{ref,fund}}$ and the positive offset voltage $v_{\text{off},p}$. Since the generated losses are reduced by the clamping region, the most aged cells are modulated with $v_{\text{ref},ns}$. The second modulation signal $v_{\text{ref},s}$, which is shown in Fig. 1(b), does not have the clamping region and is generated with the negative offset voltage $v_{\text{off},n}$ (or $-v_{\text{off},p}$) to compensate the clamping of the other cells. Hence, the offset voltages can be eliminated completely from the converter voltage by modulating the less aged cells with $v_{\text{ref},s}$ [24]. Here, the subscript ns means nonswitching and the subscript s represents switching.

Fig. 2 depicts intuitively the modulation strategy depending on the condition of each cell. As an example, one cell is showing

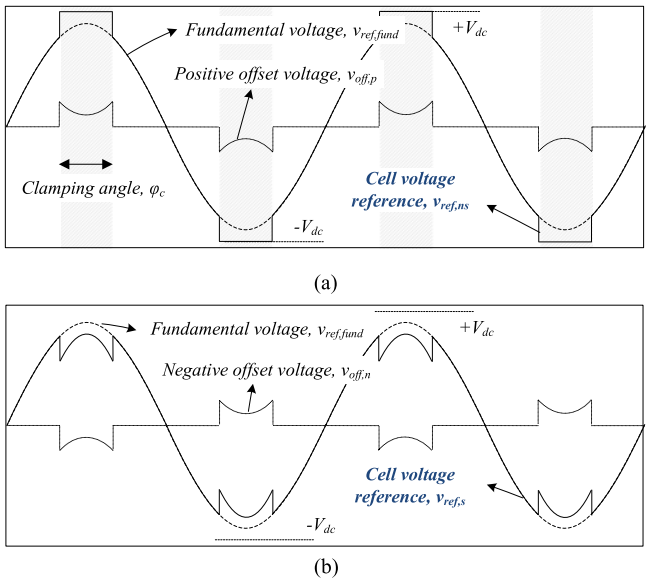

Fig. 1. Two different modes of the proposed DPWM method: (a) $v_{\text{ref},ns}$ clamping for a reduction of the switching losses and (b) $v_{\text{ref},s}$ for the compensation of the offset voltage.

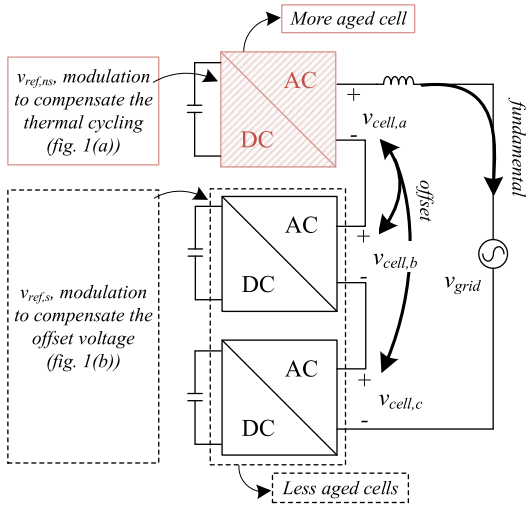

Fig. 2. Proposed modulation strategy in order to modify the thermal stress of most aged cell.

a shorter remaining useful lifetime than other two cells. The more aged cell is modulated with $v_{\text{ref},ns}$ [see Fig. 1(a)] in order to reduce its thermal stress, while the positive offset voltage is compensated by the less aged cells modulated with $v_{\text{ref},s}$ [see Fig. 1(b)].

Before finalizing this section, it should be mentioned that the $v_{\text{ref},s}$ for the compensation of the positive offset voltage cannot be used in three-phase structure since the positive offset voltages (zero sequence) are compensated by themselves.

B. Loss Distribution Among the Cells

The losses directly affect the thermal stress for the power semiconductors and the loss distribution is indentified by simulations using MATLAB/PLECS software. For the loss

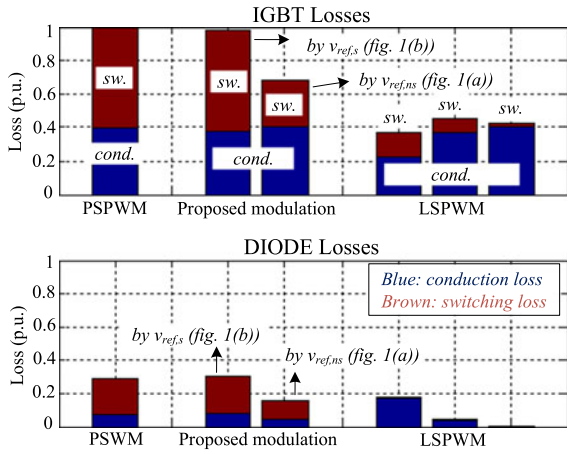

Fig. 3. Loss distribution by different modulation methods (for $P_{\rm out}$ = 100% and φ_c=60°).

model, a multidimensional lookup table is implemented for an insulated gate bipolar transistor (IGBT) power module (DP25H1200T101667) (1200 V/ 25 A) and parametrized with the experimental data obtained in [25]. Additionally, the loss model is described in the Appendix. The loss distributions for the three modulation methods (PS-PWM, LS-PWM, and the proposed method) are shown in Fig. 3 for the same carrier frequency of 23 kHz. The PS-PWM generates equal losses among cells and the highest overall losses, whereas the lowest and uneven losses are generated by the LS-PWM. As it can be expected from the Fig. 1, the proposed method has two kind of loss distributions depending on the modulation signal. The losses generated by $v_{\rm ref,s}$ are similar to that of the PS-PWM, whereas the $v_{\rm ref,ns}$ generates the reduced losses with 60° clamping angle.

In the proposed method, the clamping angle is considered as a control variable to compensate the thermal cycling and its relation to the losses is shown in Fig. 4 as a function of the output power. As shown in Fig. 4(a), the loss distribution of $v_{\rm ref,ns}$ depends not only on the output power but also on the clamping angle, while the loss distribution of $v_{\rm ref,s}$ only depends on the output power, as shown in Fig. 4(b). In fact, although the conduction losses of module modulated by $v_{\rm ref,s}$ are slightly varied, this impact on thermal stress can be negligible (see Figs. 16 and 18). Therefore, it can be concluded that this concept enables the active thermal control for the most aged cells without impacting on the others.

C. Thermal Cycling Compensation

The relation between the output power and the generated losses is shown in Fig. 5, when the clamping angle is 0° and 120°, respectively, and the losses are different in the entire power range. Therefore, the losses can be equalized within this boundary (from the minimum losses with 120° to the maximum losses with 0°) once the clamping angle is properly controlled. As an example, to equalize the loss distribution from 50% to the nominal output power, the clamping angle can be controlled. This value is called "active clamping angle" in Fig. 5 and is marked with the solid line in red. Furthermore, the active thermal

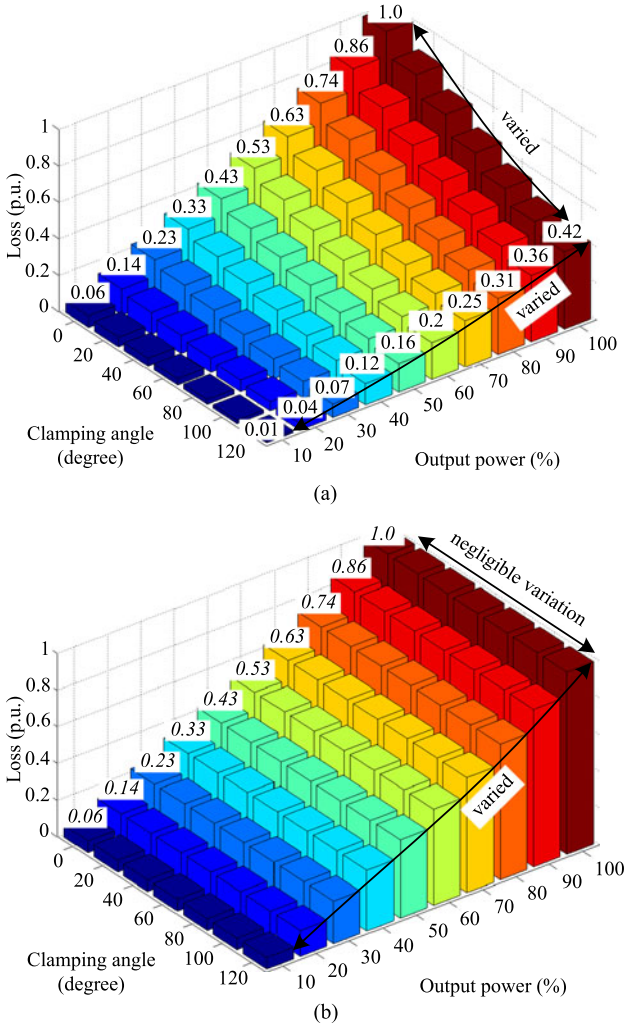

Fig. 4. Loss distribution as a function of output power and clamping angle by means of (a) $v_{\rm ref,ns}$ and (b) $v_{\rm ref,s}$.

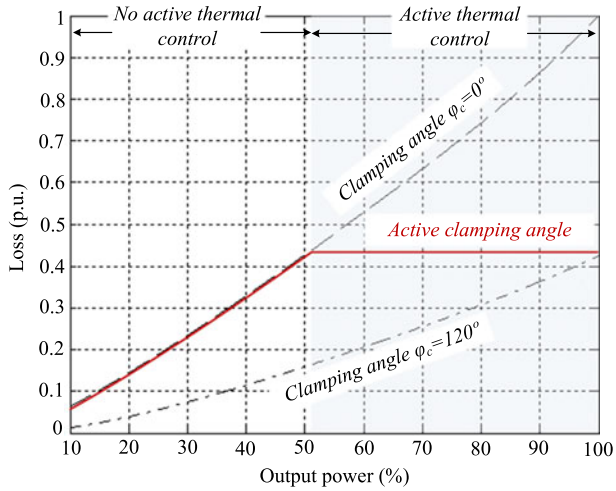

Fig. 5. Active clamping angle in order to equalize loss distribution.

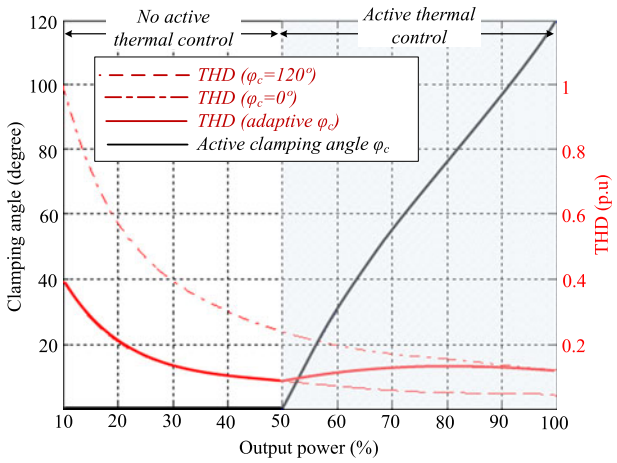

Fig. 6. THD with the active clamping angle to equalize the losses from 50% to 100% power.

control region can be set within the boundary from 27% to 60% power or from 37% to 80% as another example, depending on the most frequent condition of the mission profile.

The active clamping angle is tuned to equalize the losses from 50% to 100% power and its corresponding THD is shown in Fig. 6. The clamping angle is nonlinearly varied from 120° to 0° as the output power decreases to 50%, and below 50% power the clamping angle is set to constant 0°. Meanwhile, the THD is determined following the active clamping angle as the solid line in red.

III. Potential of the Proposed Method

A. Capability of Thermal Cycling Compensation

In order to demonstrate the effectiveness of the proposed method, its capability is benchmarked in terms of the maximum number of thermally compensated cells, considering a higher level CHB converter whose m cells are modulated by $v_{\mathrm{ref},ns}$ and the remaining n cells are operated with $v_{\mathrm{ref},s}$ (i.e., the total number of cells is $m+n$) as expressed in the following equation:

$$\begin{cases} v_{\mathrm{ref},ns(i)} = v_{\mathrm{ref,fund}} + v_{\mathrm{off},p} & (i = 1, 2, \ldots, m) \\ v_{\mathrm{ref},s(j)} = v_{\mathrm{ref,fund}} - \left(\dfrac{m}{n}\right) \cdot v_{\mathrm{off},p} & (j = 1, 2, \ldots, n) \end{cases} \tag{1}$$

where the $v_{\mathrm{ref},ns(i)}$ and the $v_{\mathrm{ref},s(j)}$ represent the modulation signals for the ith cell and the jth cell, respectively, and the m and the n are the number of cells modulated by the $v_{\mathrm{ref},ns}$ and the $v_{\mathrm{ref},s}$, respectively.

The overmodulation is the constraint for the maximum number of thermally compensated cells, since it prevents the compensation of the offset voltage ($v_{\mathrm{off},p}$), causing distorted current. Among the two modulation signals in (1), $v_{\mathrm{ref},s}$ limits the control ability due to the factor m/n. Fig. 7 exemplifies this situation: set, v_{off} is determined by the clamping angle as in (2), and with the increasing number of compensated cells the duty cycle is

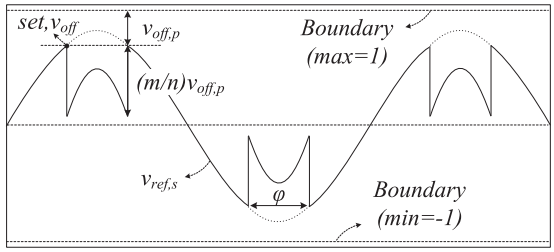

Fig. 7. Constraint of the proposed method by overmodulation of $v_{\mathrm{ref},s}$.

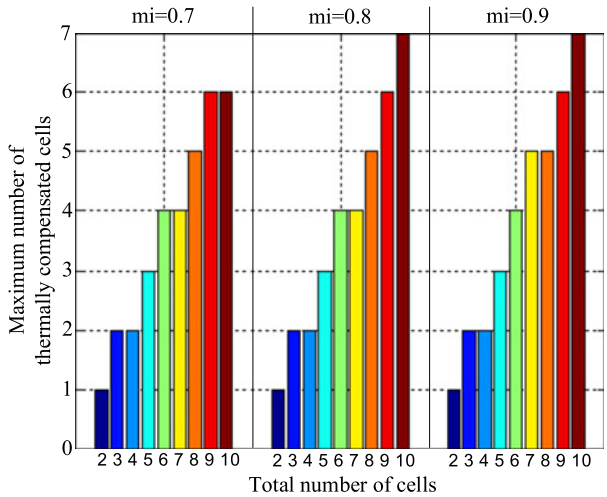

Fig. 8. Thermal compensation capability depending on the number of cells and the modulation index.

pushed toward the boundary

$$v_{\mathrm{off},p} = 1 - \mathrm{set}, v_{\mathrm{off}} = 1 - M \cdot \cos\left(\frac{\varphi}{2}\right) \tag{2}$$

where the M is the modulation index (range is from 0 to 1) and the φ is the clamping angle in degrees. Therefore, considering the number of cells (m and n) and the set point, the relation in (3) is derived, which should be satisfied to modulate the converter within the linear range

$$\begin{aligned} &\mathrm{set}, v_{\mathrm{off}} - \left(\frac{m}{n}\right) \cdot (\max - \mathrm{set}, v_{\mathrm{off}}) \geq -1 \\ &\Rightarrow \left| \left(\frac{m}{n}\right) - \left(\frac{m+n}{n}\right) \cdot \mathrm{set}, v_{\mathrm{off}} \right| \leq 1 \end{aligned} \tag{3}$$

where the left equation can be rearranged by setting $\max = 1$. Finally, by substituting (2) into (3), the maximum number of thermally compensated cells (modulated by $v_{\mathrm{ref},ns}$) is derived as a function of the total number of cells and the modulation index in Fig. 8. As it can be seen, the proposed method is further capable with the high modulation index, which implies less dc-link voltage in grid-connected converter. Therefore, this feature would be an additional advantage, since the less dc-link voltage allows the less generated losses.

B. Total Harmonic Distortion

The disadvantage of the typical DPWM is the worse THD performance, which is critical in grid-connected applications.

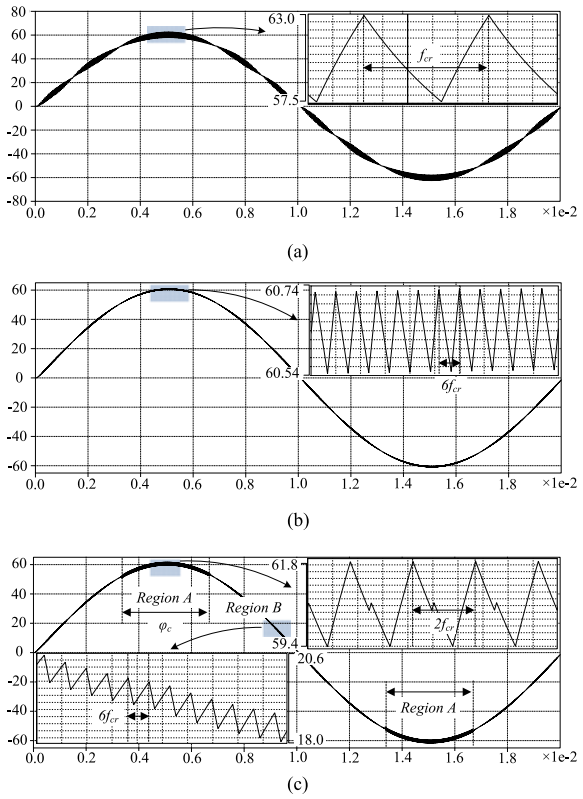

Fig. 9. Current waveform by: (a) level-shifted modulation, (b) phase-shift modulation, and (c) the proposed modulation.

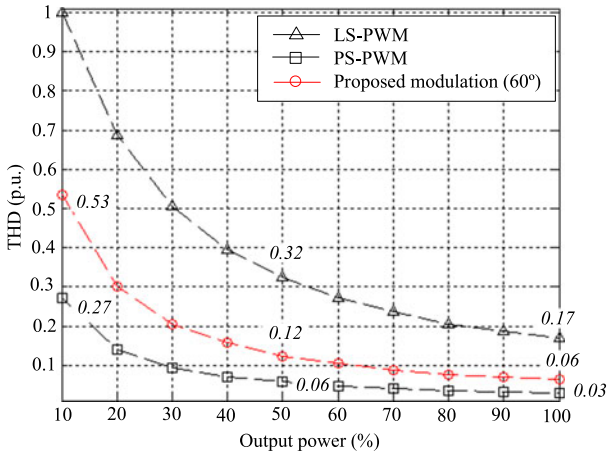

Fig. 10. Comparison of THD according to the modulation methods.

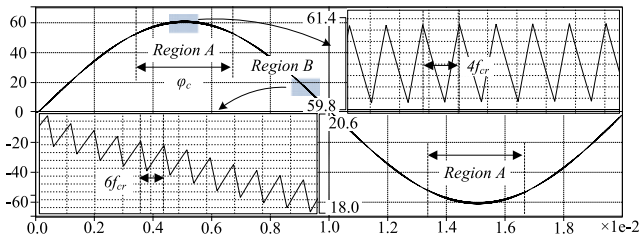

Fig. 11. Current waveform for the proposed modulation with the modified carrier.

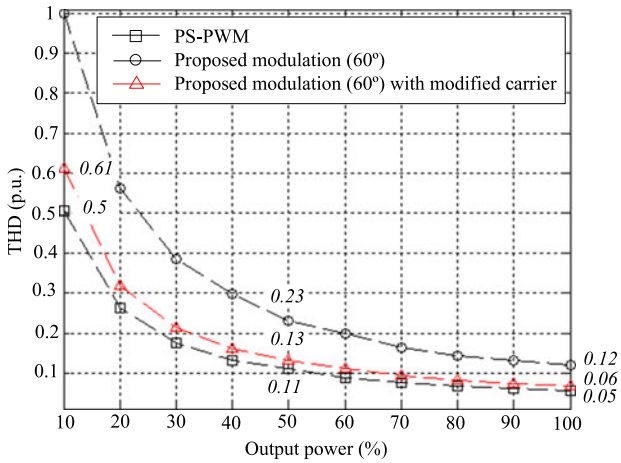

Fig. 12. Impact of the modified carrier on THD.

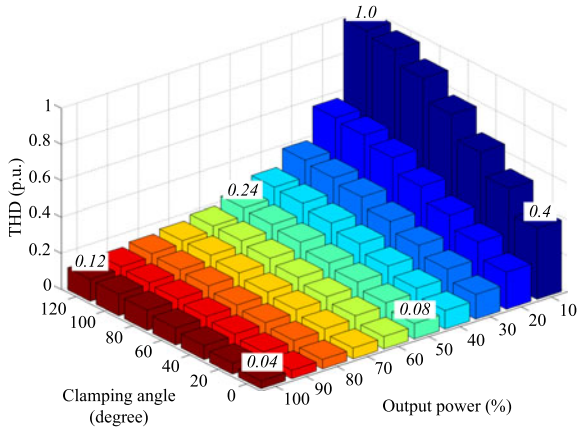

Fig. 13. THD by the proposed method with the modified carrier as a function of output power and clamping angle.

A comparison of the proposed method against the continuous one is carried on, and a possible THD improvement technique is proposed.

The current waveform with the LS-PWM, the PS-PWM, and the proposed modulation is shown in Fig. 9(a), (b), and (c), respectively. The same carrier frequency $f_{\rm cr}$ and an identical output filter are considered. For the LS-PWM, the dominant ripple frequency is equal to $f_{\rm cr}$, whereas the $6f_{\rm cr}$ dominantly appears in the current by the PS-PWM. However, as shown in Fig. 9(c), the current waveform by the proposed method can be divided into two regions: Region A (inside the clamping region) and region B (outside the clamping region). The $6f_{\rm cr}$ is dominant in the region B such as the PS-PWM, but the ripple frequency is reduced to $2f_{\rm cr}$ in the region A, which affects the THD performance. Since the proposed method adopts the carriers of PS-PWM, the equivalent switching frequency is $6f_{\rm cr}$ during the region B, where the reference signals are identical. However, during the clamping

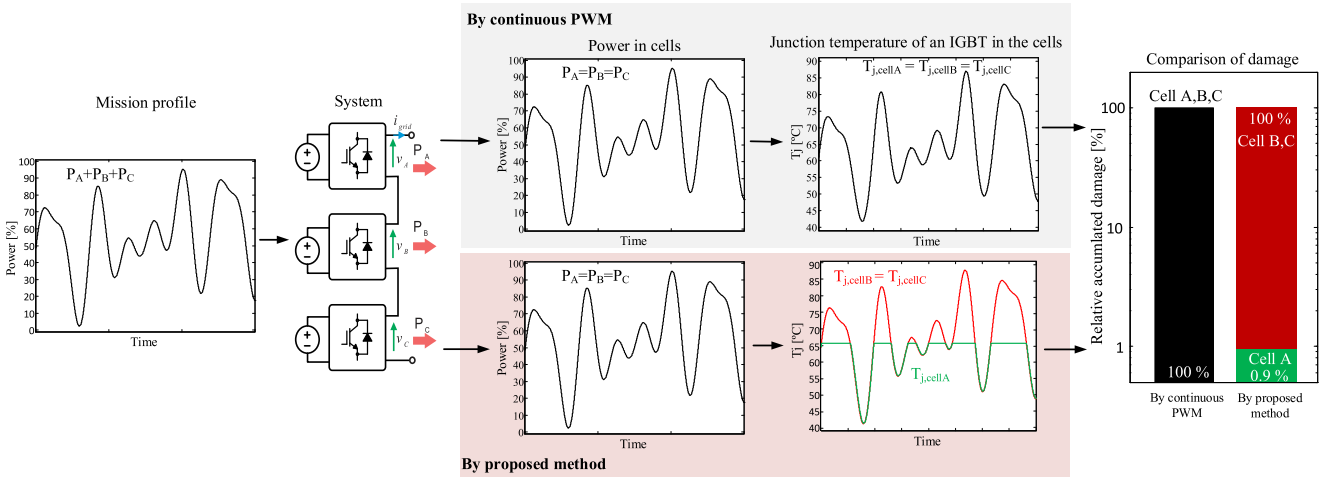

Fig. 14. Lifetime expectation of the power semiconductors depending on modulation methods: PS-PWM (top) and the proposed DPWM (bottom).

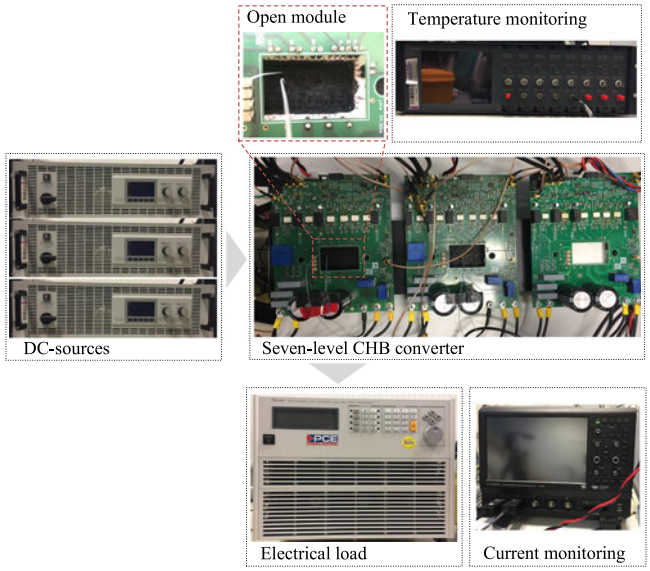

Fig. 15. Experimental setup to measure the junction temperature of IGBT modules.

region A, the equivalent switching frequency appears at $2f_{\mathrm{cr}}$ due to different reference signals among cells.

The THD of the output current for the three methods is shown in Fig 10. As expected, the LS-PWM shows the worst performance, and the best performance is achieved by the PS-PWM. At nominal power, the LS-PWM generates an approximately 5.6 times higher THD compared to the PS-PWM. The proposed method with the 60° clamping angle, gives a compromise between the two methods. Compared with the PS-PWM, the THD of the current is approximately two times higher in the entire power range.

In order to improve the THD performance for the proposed modulation, modified carriers are employed. During the clamping region, the converter can be considered as a five-level CHB by taking into account, that only two cells modulated by $v_{\mathrm{ref},s}$. Hence, the carrier signals for the two cells can be reconfigured with the 90° phase disposition instead of the 60°. The current waveform with the modified carrier is shown in Fig. 11, where the frequency of the current ripple during the clamping region is increased to $4f_{\mathrm{cr}}$. The effect of the modified carrier on the THD is demonstrated in Fig. 12. For the proposed method, the THD of the output current is reduced to $50\,\%$ in comparison with the case without the modified carrier and it is comparable with that of the PS-PWM.

Finally, the THD of the current is shown for the proposed method in Fig. 13 as a function of the output power and the clamping angle. As the clamping angle increases, its THD decreases approximately 2.5–3 times between 0° and 120°.

IV. Reliability Impact of the Proposed Method

To give an estimation about the reliability impact of the proposed, this section applies a common lifetime model for power semiconductors in power modules. This considers the failure mechanisms of bond wire liftoff, which is caused by the temperature variations and temperature gradients in the modules. It has been found empirically that the number of cycles to failure N_f can be estimated in dependence of the average temperature $T_{j,\mathrm{mean}}$ and the thermal cycling ΔT_j [10]

$$N_f = a_1 \cdot (\Delta T_j)^{-a_2} \cdot e^{\frac{a_3}{T_{j,\mathrm{mean}}}}. \tag{4}$$

In this equation, a_1 and a_2 are parameters determined by experimental data and related with physical characteristics of a power semiconductor, and a_3 is a constant, which can be calculated with the activation energy and the Boltzmann constant. This lifetime model expressed with (1) only considers a single thermal cycle magnitude, which is not sufficient to be applied in a real mission profile. In this case, there are many thermal cycles, which superimpose each others. As a solution to detect these cycles, Rainflow counting in commonly applied to extract the thermal cycles from the mission profile in dependence of their magnitude [26]. Based on this result, linear damage

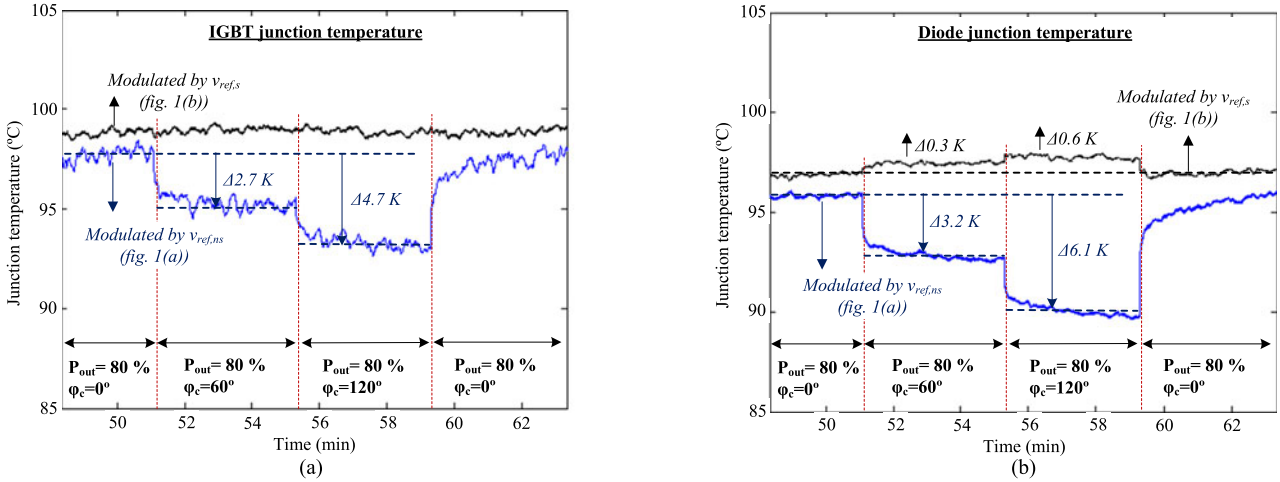

Fig. 16. Impact of the clamping angle on the junction temperature of (a) IGBT and (b) freewheeling diode ($P_{\rm out} = 80$ %).

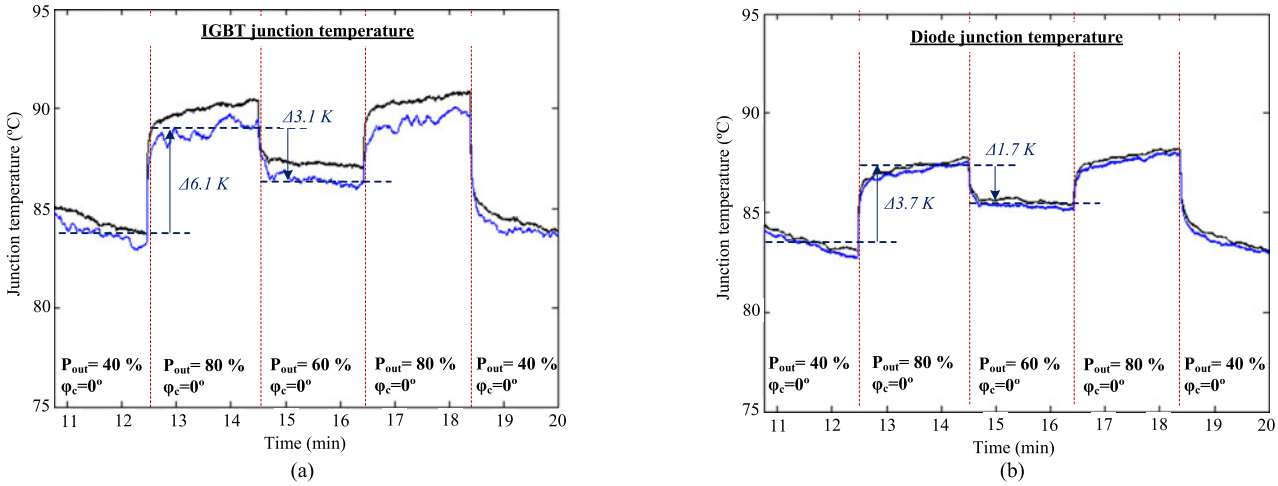

Fig. 17. Variation of (a) IGBT and (b) freewheeling diode junction temperature in accordance with output power ($\varphi_c = 0°$).

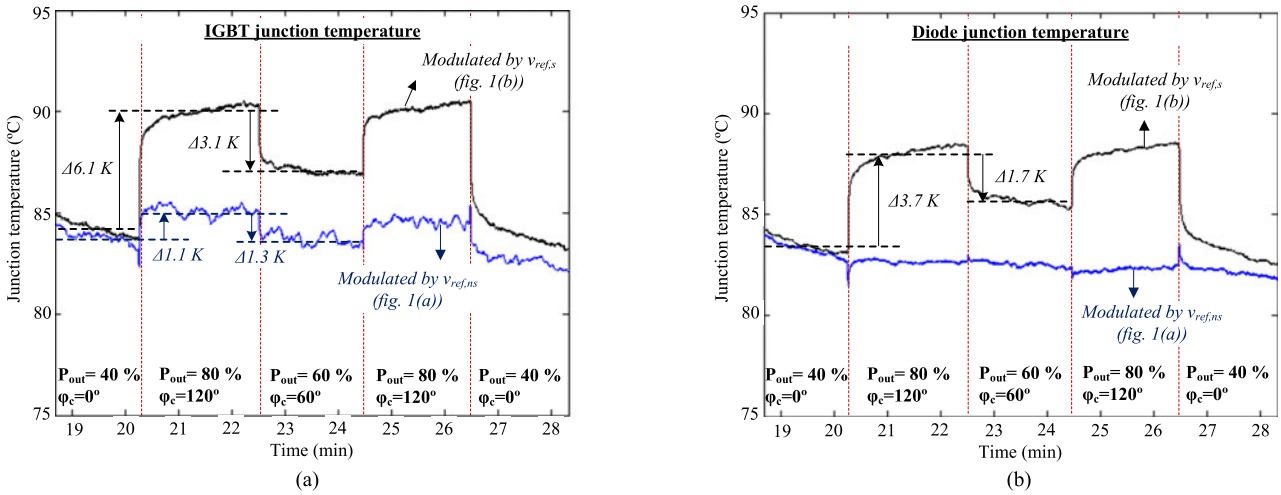

Fig. 18. Compesation of (a) IGBT and (b) freewheeling diode junction temperature by the active clamping angle.

accumulation can be calculated with Miner's rule [27]

$$C = \sum_{i=0}^{\inf} \frac{n_i}{N_i} \leq 1. \tag{5}$$

In this equation, N_i is the number of cycles to failure in the stress range i and n_i the number of detected cycles in the ith stress range. As soon as the accumulated damage reaches $C = 1$, the device is expected to fail.

This model is applied to give an estimation of the increase in lifetime, if the proposed method is applied. A mission profile with fluctuating power is used, as shown in Fig. 14. A constant ambient temperature $T_a = 40\,^{\circ}\mathrm{C}$ and a design for the maximum junction temperature of $T_{j,\max} = 90\,^{\circ}\mathrm{C}$ is assumed. In the first case the cells are loaded equally, while in the second case the active clamping period is used, as shown in Fig. 5. The clamping angle is set to $\varphi_c = 0\,^{\circ}$ for an output power lower than 50%, while it is adapted to hold the junction temperature constant for power higher than 50%. This results in less junction temperature fluctuation for a power semiconductor in the cell, which is clamping the angle as it can be seen for cell A. To quantify the reduction in thermal stress, rainflow counting is applied and linear damage accumulation is made. It can be seen that the damage for the cell A is reduced to approximately $1\,\%$ of the prior damage, while the other cells keep their damage unchanged. Consequently, an expected lifetime increase for the cell A by a factor of 100 is achieved.

V. Experimental Results

In this section, the proposed method is validated by measuring the junction temperature of a power module. The developed prototype shown in Fig. 15 is composed of the seven-level CHB converter with open power modules, a temperature and current monitoring system, an electrical load, and dc sources. The specification of power modules is 1200 V/25 A (Part number: DP25H1200T101667), 23-kHz carrier frequency is utilized and the total dc-link voltage of 450 V is applied (150 V for each cell). Although the operating voltage is below the rated one, the devices still undergo thermal stress, making the setup valid for demonstration purpose. Finally, the junction temperature is directly measured by fiber optic sensors "OTG-F" and signal conditioner "ProSens."

The impact of the clamping angle is presented in Fig. 16, with a fixed power at 80%. As mentioned in Section II-B (see Fig. 4), the junction temperature of the cell operated with $v_{\mathrm{ref},ns}$ is influenced by the clamping angle. The IGBT junction temperature is reduced approximately by 2.7 K with the 60° clamping angle and 4.7 K with the 120° clamping angle, while for the freewheeling diode, the temperature decreases approximately by 3.2 and 6.1 K with 60° and 120° clamping angle, respectively. On the other hand, the influence on the junction temperature of the cell modulated by $v_{\mathrm{ref},s}$ is negligible (here, the small variation in the freewheeling diode is due to the slightly increased conduction losses as mentioned in Section II-B). This result matches well with the loss distribution analysis.

The temperature variation is dependent on the output power as presented in Fig. 17, where the clamping angle is set to 0°. The temperature is reduced by 6.1 and 3.7 K in the IGBT and diode, respectively, with the power changed from 40% to 80%, whereas 3.1 and 1.7 K is changed when the power is reduced from 80% to 60%. With the above temperature profile in Figs. 16 and 17, it is expected that the temperature variation due to the power change can be compensated with the different clamping angle as claimed in Section II.

Finally, the active clamping angle is adopted to compensate the junction temperature variation at different powers, as shown in Fig. 18. While the temperature of the cell operated with the $v_{\mathrm{ref},ns}$ is compensated, another cell modulated by the $v_{\mathrm{ref},s}$ shows a similar temperature profile to Fig. 17. In the compensated profile in Fig. 18, the temperature of the IGBT is reduced by 79% (power changed from 40% to 80%) and by 64% (power changed from 60% to 80%), as shown in Fig. 18(a), while the temperature variation on the diode is almost equalized, as shown in Fig. 18(b).

VI. Conclusion

This paper presented the modulation strategy based on the discontinuous modulation for the cascaded H-bridge converter. Considering an unequal remaining lifetime among cells, this method enables reducing the thermal stress of more aged cells. The effect of the method on the lifetime extension was verified by simulations, showing that a damage reduction up to 99% under the considered power profile can be achieved. The thermal compensation limits of the proposed method were presented and the performance of the THD shows results, which are similar to the phase-shift modulation. Finally, the proposed method was experimentally validated in a proof-of-concept setup with open power modules by measuring the device junction temperature. The laboratory tests confirmed the thermal compensation capability of the proposed method.

Appendix
PLECS: Loss Simulation Model

The loss simulation of MATLAB/PLECS is based on the multidimensional lookup table approach, with the information provided in the datasheet of the manufacturer or obtained by experiments. The lookup table for switching losses is a function of the current, the blocking voltage, and the junction temperature. The conduction losses are calculated based on second order approximation of the current and the junction temperature is taken into account as well.

In this paper, the lookup table was populated using the experimental results obtained in [25]. The power module (DP25H1200T101667) was characterized with 400 Vdc and the used loss model is shown in Fig. A-1. For the IGBT model, the switching losses (turn-on and turn-off) and the conduction losses are considered, whereas the turn-on losses are ignored for the diode model since this is relatively negligible.

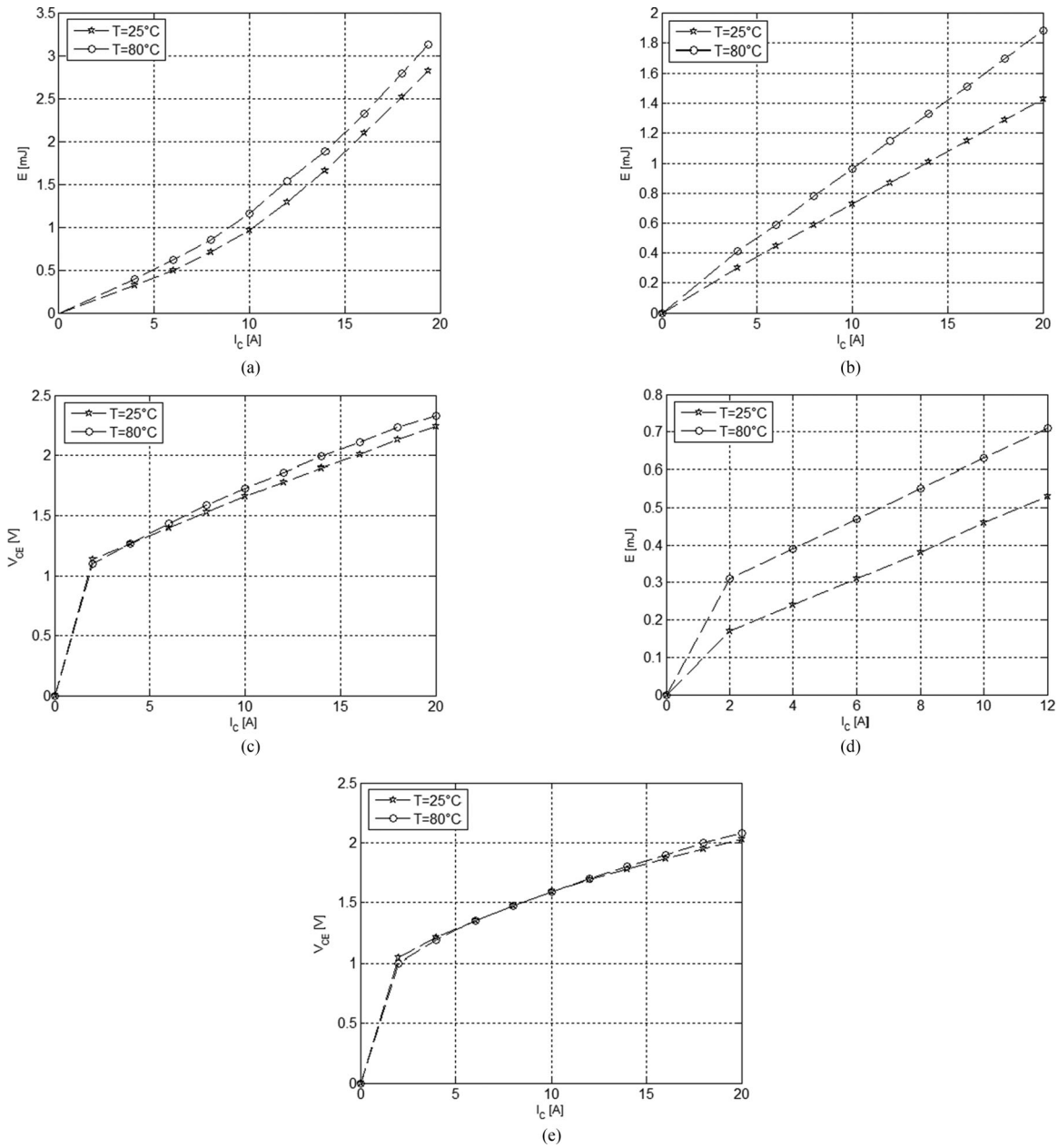

Fig. A-1. Loss model; (a) IGBT turn-on, (b) IGBT turn-off, (c) IGBT conduction, (d) Diode turn-off, and (e) Diode conduction.

REFERENCES

[1] M. R. Islam, Y. Guo, and J. Zhu, "A multilevel medium-voltage inverter for step-up-transformer-less grid connection of photovoltaic power plants," *IEEE J. Photovolt.*, vol. 4, no. 3, pp. 881–889, May 2014.

[2] M. Wang, Y. Hu, W. Zhao, Y. Wang, and G. Chen, "Application of modular multilevel converter in medium voltage high power permanent magnet synchronous generator wind energy conversion systems," *IET Renewable Power Gener.*, vol. 10, no. 6, pp. 824–833, 2016.

[3] N. Thitichaiworakorn, M. Hagiwara, and H. Akagi, "A medium-voltage large wind turbine generation system using an ac/ac modular multilevel cascade converter," *IEEE J. Emerg. Sel. Topics Power Electron.*, vol. 4, no. 2, pp. 534–546, Jun. 2016.

[4] B. Wu, *Cascaded H-Bridge Multilevel Inverters*. Hoboken, NJ, USA: Wiley, 2006, pp. 119–142. [Online]. Available: http://ieeexplore.ieee.org/xpl/articleDetails.jsp?arnumber=5238047

[5] A. Edpuganti and A. K. Rathore, "A survey of low switching frequency modulation techniques for medium-voltage multilevel converters," *IEEE Trans. Ind. Appl.*, vol. 51, no. 5, pp. 4212–4228, Sep. 2015.

[6] J. Rodriguez, J.-S. Lai, and F. Z. Peng, "Multilevel inverters: A survey of topologies, controls, and applications," *IEEE Trans. Ind. Electron.*, vol. 49, no. 4, pp. 724–738, Aug. 2002.

[7] M. Malinowski, K. Gopakumar, J. Rodriguez, and M. A. Perez, "A survey on cascaded multilevel inverters," *IEEE Trans. Ind. Electron.*, vol. 57, no. 7, pp. 2197–2206, Jul. 2010.

[8] E. Babaei, M. Sarbanzadeh, M. A. Hosseinzadeh, and C. Buccella, "A new topology for cascaded multilevel inverters with reduced number of power electronic switches," in *Proc. 2016 7th Power Electron. Drive Syst. Technologies Conf.*, Feb. 2016, pp. 165–170.

[9] H. Wang *et al.*, "Transitioning to physics-of-failure as a reliability driver in power electronics," *IEEE J. Emerg. Sel. Topics Power Electron.*, vol. 2, no. 1, pp. 97–114, Mar. 2014.

[10] M. Held, P. Jacob, G. Nicoletti, P. Scacco, and M. H. Poech, "Fast power cycling test of IGBT modules in traction application," in *Proc. 2nd Int. Conf. Power Electron. Drive Syst.*, vol. 1, May 1997, pp. 425–430.

[11] K. Ma, M. Liserre, F. Blaabjerg, and T. Kerekes, "Thermal loading and lifetime estimation for power device considering mission profiles in wind power converter," *IEEE Trans. Power Electron.*, vol. 30, no. 2, pp. 590–602, Feb. 2015.

[12] N. C. Sintamarean, F. Blaabjerg, H. Wang, F. Iannuzzo, and P. de Place Rimmen, "Reliability oriented design tool for the new generation of grid connected pv-inverters," *IEEE Trans. Power Electron.*, vol. 30, no. 5, pp. 2635–2644, May 2015.
[13] C. Durand, M. Klingler, D. Coutellier, and H. Naceur, "Power cycling reliability of power module: A survey," *IEEE Trans. Device Mater. Reliab.*, vol. 16, no. 1, pp. 80–97, Mar. 2016.
[14] M. Andresen, M. Liserre, and G. Buticchi, "Review of active thermal and lifetime control techniques for power electronic modules," in *Proc. 2014 16th Eur. Conf. Power Electron. Appl.*, Aug. 2014, pp. 1–10.
[15] D. A. Murdock, J. E. R. Torres, J. J. Connors, and R. D. Lorenz, "Active thermal control of power electronic modules," *IEEE Trans. Ind. Appl.*, vol. 42, no. 2, pp. 552–558, Mar. 2006.
[16] M. Andresen, G. Buticchi, J. Falck, M. Liserre, and O. Muehlfeld, "Active thermal management for a single-phase H-bridge inverter employing switching frequency control," in *Proc. Int. Exhib. Conf. Power Electron., Intell. Motion, Renew. Energy Energy Manage., Proc. PCIM Eur.*, May 2015, pp. 1–8.
[17] J. Falck, M. Andresen, and M. Liserre, "Active thermal control of IGBT power electronic converters," in *Proc. 41st Annu. Conf. IEEE Ind. Electron.*, Nov. 2015, pp. 1–6.
[18] M. Liserre, M. Andresen, L. Costa, and G. Buticchi, "Power routing in modular smart transformers: Active thermal control through uneven loading of cells," *IEEE Ind. Electron. Mag.*, vol. 10, no. 3, pp. 43–53, Sep. 2016.
[19] Y. Ko, M. Andresen, G. Buticchi, and M. Liserre, "Power routing for cascaded h-bridge converters," *IEEE Trans. Power Electron.*, 2017.
[20] L. Wei, J. M. C. Guire, and J. Hu, "Novel discontinuous PWM control method to improve IGBT reliability at low speed," in *Proc. 2014 IEEE Energy Convers. Congr. Expo.*, Sep. 2014, pp. 3819–3825.
[21] A. Isidori, F. M. Rossi, F. Blaabjerg, and K. Ma, "Thermal loading and reliability of 10-MW multilevel wind power converter at different wind roughness classes," *IEEE Trans. Ind. Appl.*, vol. 50, no. 1, pp. 484–494, Jan. 2014.
[22] A. M. Hava, R. J. Kerkman, and T. A. Lipo, "A high-performance generalized discontinuous PWM algorithm," *IEEE Trans. Ind. Appl.*, vol. 34, no. 5, pp. 1059–1071, Sep. 1998.
[23] L. Dalessandro, S. D. Round, U. Drofenik, and J. W. Kolar, "Discontinuous space-vector modulation for three-level PWM rectifiers," *IEEE Trans. Power Electron.*, vol. 23, no. 2, pp. 530–542, Mar. 2008.
[24] Y. Ko, M. Andrsen, G. Buticchi, J. S. Lee, and M. Liserre, "Modulation strategy for highly reliable cascade H-bridge inverter based on discontinuous PWM," in *Proc. 2017 IEEE Appl. Power Electron. Conf. Expo.*, 2017.
[25] M. Andresen, M. Schloh, G. Buticchi, and M. Liserre, "Computational light junction temperature estimator for active thermal control," in *Proc. 2016 IEEE Energy Convers. Congr. Expo.*, Sep. 2016, pp. 1–7.
[26] M. Musallam and C. M. Johnson, "An efficient implementation of the rainflow counting algorithm for life consumption estimation," *IEEE Trans. Reliab.*, vol. 61, no. 4, pp. 978–986, Dec. 2012.
[27] M. Musallam, C. Yin, C. Bailey, and M. Johnson, "Mission profile-based reliability design and real-time life consumption estimation in power electronics," *IEEE Trans. Power Electron.*, vol. 30, no. 5, pp. 2601–2613, May 2015.

Youngjong Ko (S'16) received the B.Sc. and M.Sc. degrees in electronic engineering from Ajou University, Suwon, South Korea, in 2009 and 2012, respectively. Since 2015, he has been working toward the Ph.D. degree at the Chair of Power Electronics, University of Kiel, Kiel, Germany.

His research interests include grid-connected power converter and reliability in power electronics.

Markus Andresen (S'15) received the M.Sc. degree in electrical engineering and business administration, in 2012, from Christian-Albrechts-University of Kiel, Kiel, Germany, where he has been working toward the Ph.D. degree at the Chair of Power Electronics since 2013.

In 2010, he was an Intern in the Delta Shanghai Design Center, Delta Electronics (Shanghai) Co., Ltd., China, and in 2017, he was a Visiting Scholar in the University of Wisconsin-Madison, Madison, WI, USA. His current research interests include control of power converters and reliability in power electronics.

Giampaolo Buticchi (S'10–M'13–SM'17) was born in Parma, Italy, in 1985. He received the master's degree in electronic engineering, in 2009, and the Ph.D. degree in information technologies from the University of Parma, Parma, Italy, in 2013.

In 2012, he was Visiting Researcher in The University of Nottingham, Nottingham, U.K. He is currently a Postdoctoral Research Associate at the University of Kiel, Kiel, Germany. His research interests include power electronics for renewable energy systems, smart transformer fed microgrids, and reliability in power electronics.

Marco Liserre (S'00–M'02–SM'07–F'13) received the M.Sc. and Ph.D. degrees in electrical engineering from the Bari Polytechnic, Bari, Italy, 1998 and 2002, respectively.

He was an Associate Professor in Bari Polytechnic and a Professor in reliable power electronics in Aalborg University, Aalborg, Denmark. He is currently a Full Professor and the Chair of Power Electronics at Christian-Albrechts-University of Kiel, Kiel, Germany. He has published more than 300 technical papers (more than 70 of them in international peer-reviewed journals), four chapters of a book and a book: *Grid Converters for Photovoltaic and Wind Power Systems* (Wiley, second reprint, also translated in Chinese). These works have received more than 20000 citations.

Prof. Liserre is listed in ISI Thomson report "The world's most influential scientific minds" from 2014. He received an ERC Consolidator Grant for the project "The Highly Efficient And Reliable smart Transformer (HEART), a new Heart for the Electric Distribution System." He has received the IES 2009 Early Career Award, the IES 2011 Anthony J. Hornfeck Service Award, the 2014 Dr. Bimal Bose Energy Systems Award, the 2011 Industrial Electronics Magazine best paper award, and the Third Prize Paper Award by the Industrial Power Converter Committee at ECCE 2012. He is a member of IAS, PELS, PES, and IES. He is senior member of IES AdCom. He is also an Associate Editor of the IEEE TRANSACTIONS ON INDUSTRIAL ELECTRONICS, the IEEE INDUSTRIAL ELECTRONICS MAGAZINE, the IEEE TRANSACTIONS ON INDUSTRIAL INFORMATICS, where he is currently Co-Editor-in-chief, the IEEE TRANSACTIONS ON POWER ELECTRONICS and the IEEE JOURNAL OF EMERGING AND SELECTED TOPICS IN POWER ELECTRONICS. He has been Founder and Editor-in-Chief of the IEEE INDUSTRIAL ELECTRONICS MAGAZINE, the Founder and the Chairman of the Technical Committee on Renewable Energy Systems, the Co-Chairman of the International Symposium on Industrial Electronics (2010), and the IES Vice-President responsible of the publications. In 2013, he has been elevated to the IEEE Fellow grade with the following citation "for contributions to grid connection of renewable energy systems and industrial drives."